Pergamon

Int. J. Solids Structures Vol. 34, Nos 33–34, pp. 4327–4337, 1997

0020-7683/97 $17.00 + .00

PII: S0020-7683(97)00027-9

A MODIFIED FOURIER SERIES METHOD FOR THE TORSION ANALYSIS OF BARS WITH MULTIPLY CONNECTED CROSS SECTIONS

YOON YOUNG KIM and MIN SU YOON
Department of Mechanical Design and Production Engineering, Seoul National University, Kwanak-Gu, Shinlim-Dong, San 56-1, Seoul 151-742, Korea

(*Received* 6 *August* 1996; *in revised form* 26 *December* 1996)

Abstract—A modified Fourier series method is proposed for the torsion analysis of prismatic bars with multiply connected cross sections. The key feature in the present approach is the combined use of polynomials and Fourier series solutions unlike in the existing approaches which use the Fourier series only. The replacement of the zeroth harmonic terms in the Fourier series solutions by carefully selected polynomials resolves the major problem of functional dependence which the direct Fourier series method may pose. The polynomials and Fourier series solutions are selected to satisfy the governing equation exactly so that the numerical calculation is minimal. The effectiveness and generality of the present method is verified through numerical examples. © 1997 Elsevier Science Ltd.

1. INTRODUCTION

In the analysis of beam structures, the sectional properties such as bending and torsional rigidities, and the magnitude and location of the maximum stress are usually of primary interest. In the case of non-circular cylindrical beams subjected to twisting, the strength-of-material solutions cannot be used, and the warping of the cross section must be considered.

Although the exact solutions for warping of beams are available for some simple geometries (Timoshenko, 1982), no closed-form solutions are possible for general cross sections. Subsequently, several alternative analytical (Irschik, 1991; Rand, 1992) as well as numerical (Mason and Herrmann, 1968; Ie and Kosmatka, 1992) methods are proposed.

Since the warping problems can be formulated with Laplace's or Poisson's equation, it is worthwhile to review work done on the solution methods on these equations. Among others, Bird and Steele (1992) proposed an efficient Fourier series method to solve Laplace's equation in regions bounded only by circles. A similar effective approach for more general geometries, has been developed by Kang (1992) and Kang *et al.* (1995) for polygonal plate bending.

The technique by Kang (1992) and Kang *et al.* (1995), utilizing the Fourier series solutions alone, can be applied to the present problem. In their formulation, however, the governing Laplace equation is approximated as the Helmholtz equation with a small parameter which is somewhat arbitrary; Laplace's equation cannot be solved directly with his approach. This is due to the difficulty in treating the series terms associated with the zeroth harmonics. In terms of computational efficiency, however, the technique is powerful as the Fourier series solutions satisfy the Helmholtz equation exactly.

In this paper, we propose a modified Fourier series method for the torsion analysis of bars with multiply connected cross sections bounded by straight edges. The present technique also utilizes the Fourier series solutions, but carefully selected low-order polynomials, which satisfy the governing equation, are also employed. More specifically, we replace the typical series solutions associated with the zeroth harmonics with the present polynomials; the former cannot represent global deformation with non-vanishing resultants, but the latter can. Therefore, the governing differential equation, Laplace's equation, is directly solved with this modification and thus the use of the artificial parameter suggested by earlier investigations (Kang, 1992; Kang *et al.*, 1995) is avoided.

We remark that the significance of the use of polynomials instead of typical zeroth harmonic series solutions has not been reported in the existing literature, and that the correct form of the polynomials is presented here for the first time. The present method is given first for simply connected convex cross sections and then extended to multiply connected general cross sections. Its effectiveness and accuracy is examined by comparing the present results with exact, or the ANSYS finite element results.

2. FORMULATION WITH THE WARPING FUNCTION

The torsional problems in prismatic bars are often formulated in terms of the Prandtl stress function, which satisfies Poisson's equation (Sokolnikoff, 1956). Due to the analogy between the Prandtl stress function and the deflection of a membrane under uniform pressure, the stress function formulation has been preferred by several investigators. Alternatively, the function representing the warping displacement, which satisfies Laplace's equation, can be also used. The advantage of using the direct warping function is that no extra compatibility condition is needed in bars of general cross sections and the warping displacement can be directly obtained from the warping function. Because of these, the warping function formulation will be employed in the present work.

If in-plane displacements are denoted by u and v, and the warping displacement by w in a beam, then

$$u(x,y,z) = -\alpha zy; \quad v(x,y,z) = \alpha zx; \quad w(x,y,z) = \alpha\phi(x,y) \tag{1}$$

where the warping function ϕ satisfies Laplace's equation (Sokolnikoff, 1956):

$$\nabla^2\phi(x,y) = 0. \tag{2}$$

In eqn (1), x, y, z are the Cartesian coordinates, and α is the angle of twist per unit length along the z axis. The shear stress components are then expressed as

$$\sigma_{zy} = G\alpha\left(\frac{\partial\phi}{\partial y}+x\right); \quad \sigma_{zx} = G\alpha\left(\frac{\partial\phi}{\partial x}-y\right) \tag{3}$$

where G denotes the shear modulus.

The traction-free lateral surface condition can be expressed as

$$\frac{\mathrm{d}\phi}{\mathrm{d}v} = yv_x - xv_y \tag{4}$$

and (v_x, v_y) is the outward unit normal vector along the boundary curve C of the cross section. From eqn (2) or eqn (4), it is straightforward to obtain

$$\int_C \frac{\partial\phi}{\partial v}\mathrm{d}s = 0. \tag{5}$$

When the torsion problem is formulated in terms of the warping function ϕ, eqn (5) is not to be imposed explicitly. However, eqn (5) may be used as a criterion to check the validity of any solution method.

Utilizing eqn (3), the torsional rigidity D can be written as

$$D = G\left[\iint_R (x^2+y^2)\,\mathrm{d}A + \iint_R \left(x\frac{\partial\phi}{\partial y} - y\frac{\partial\phi}{\partial x}\right)\mathrm{d}A\right]. \tag{6}$$

In eqn (6), the first integral over the cross sectional region R is simply the polar moment of

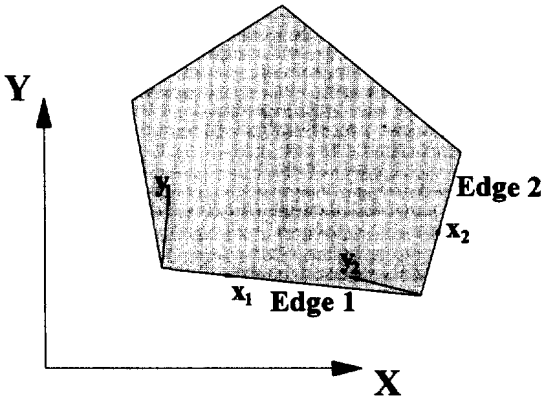

Fig. 1. The geometry of a convex polygon. The local Cartesian coordinates (x_i, y_i) are introduced at each edge.

inertia, and the second integral accounts for the contribution from the warping effect. In the numerical calculation of D, it is convenient, particularly in polygonal regions, to transform the two integrals in eqn (6) into the following line integrals:

$$\iint_R (x^2+y^2)\,\mathrm{d}A = \int_C (f\,\mathrm{d}x+g\,\mathrm{d}y) \tag{7a}$$

$$\iint_R \left(x\frac{\partial\phi}{\partial y}-y\frac{\partial\phi}{\partial x}\right)\mathrm{d}A = -\int_C \phi\left(\frac{\partial\phi}{\partial v}\right)\mathrm{d}s \tag{7b}$$

where we may take $f=-y^3/3$, and $g=x^3/3$ although other combinations of f and g are possible. The line integral in eqn (7a) can be obtained in closed form for polygonal regions, and the line integral in eqn (7b) is particularly useful when ϕ and $\partial\phi/\partial v$ are known on the boundary C.

3. SOLUTION METHOD FOR CONVEX POLYGONAL CROSS SECTIONS

The present technique for the convex polygonal cross sections will be described in this section, and the extension to general multiply connected cross sections will then follow in the next section.

Among various ways to express the boundary conditions (either ϕ or $\mathrm{d}\phi/\mathrm{d}v$), one may choose to express them in terms of the Fourier cosine series:

$$\phi^{(i)}(x_i, y_i=0) = \tilde{W}_0^{(i)} + \sum_{n=1}^{N_h} \tilde{W}_n^{(i)} \cos\frac{n\pi}{L_i}x_i \quad (i=1,\ldots,N_s) \tag{8}$$

$$L_i\frac{\mathrm{d}\phi^{(i)}}{\mathrm{d}v}(x_i, y_i=0) = \frac{\tilde{F}_0^{(i)}}{2} + \sum_{n=1}^{N_h} \tilde{F}_n^{(i)} \cos\frac{n\pi}{L_i}x_i \quad (i=1,\ldots,N_s). \tag{9}$$

In eqns (8, 9), the local Cartesian coordinates x_i and y_i, shown in Fig. 1, are associated with the ith edge of length L_i and N_s is the total number of edges. The nth Fourier coefficients along the ith edge are denoted by $\tilde{W}_n^{(i)}$ and $\tilde{F}_n^{(i)}$, and N_h is the highest term in the series. The

relation between (x_i, y_i) and the global Cartesian coordinates (X, Y) can be easily obtained:

$$\begin{Bmatrix} x_i \\ y_i \end{Bmatrix} = \mathbf{R}_i \begin{Bmatrix} X - X_i \\ Y - Y_i \end{Bmatrix}; \quad \mathbf{R}_i = \begin{bmatrix} \cos\theta_i & -\sin\theta_i \\ \sin\theta_i & \cos\theta_i \end{bmatrix}$$

where X_i and Y_i are the global coordinates of the ith vertex and θ_i is the angle between the ith edge and the X-axis.

The superscript $\tilde{}$ in eqns (8, 9) is used to emphasize the quantities associated with the boundary. Since $\tilde{F}_n^{(i)}$ are defined as the series coefficients of $L_i \partial\phi^{(i)}/\partial v$ instead of $\partial\phi^{(i)}/\partial v$, and the scaling factor of 1/2 is used in the definition of the zeroth coefficient, the expression for the virtual edge work is shown to be the following simple form†:

$$\delta E^{(i)} = G \sum_{i=1}^{N_s} \int \frac{\partial \phi^{(i)}}{\partial v} \cdot \delta\phi^{(i)} \, \mathrm{d}s = G \sum_{i=1}^{N_s} \frac{1}{2} \sum_{n=1}^{N_h} \tilde{F}_n^{(i)} \, \delta \tilde{W}_n^{(i)}. \tag{10}$$

Guided by the form of the boundary conditions expressed as eqns (8, 9), one may adopt the following base functions in a solution procedure:

$$\phi(x, y) = \sum_{i=1}^{N_s} \phi^{(i)}(x_i, y_i) \tag{11a}$$

$$\phi^{(i)}(x_i, y_i) = \sum_{n=0}^{N_h} A_n^{(i)} \cos\frac{n\pi}{L_i} x_i \exp\left(-\frac{n\pi}{L_i} y_i\right) \quad (i = 1, \ldots, N_s). \tag{11b}$$

The nature of these functions is that

(1) they satisfy the governing differential equation exactly,
(2) the period of the series is $2L_i$ where L_i is the ith edge length,
(3) the functions $\phi^{(i)}$ represent end effects decaying away from the boundary of the half space (with $y_i \geqslant 0$).

Since these base functions satisfy the governing differential equation exactly, any method based on these functions would require minimal numerical calculation. However, the serious defect in using the base functions (11b) alone is that the terms with $n = 0$ do not contribute to $\tilde{F}_0^{(i)}$ of the boundary condition and, other terms with $n \neq 0$ represent only end-effect solutions. Therefore, it is clear that eqn (11b) alone cannot be used to solve Laplace's equation for general boundary conditions.

This problem was observed in Kang (1992) and Kang *et al.* (1995), and an attempt to circumvent this problem was made by approximating Laplace's equation as

$$\nabla^2\phi - k\phi = 0 \tag{12}$$

rather than finding the correct base functions. They approximated Laplace's equation by eqn (12) with a very small number of k (but $k \neq 0$), and constructed the functions similar to (11). Although this technique was quite successful, the choice of the small parameter k is determined by trial and error.

The purpose of the present work is to find an efficient method to solve Laplace's equation directly without introducing the small numerical parameter k as in eqn (12). To this end, we carefully reexamine the base functions $\phi^{(i)}$ in eqn (11b). Then it is found that the terms with $n = 0$ (for $i = 1, \ldots, N_s$) in eqn (11b), which give constant values, are not functionally independent and produce zero values of $\partial\phi/\partial v$. In other words, the base functions (11b) for $n = 0$, when superposed for all i's, are neither independent, nor sufficient to handle the boundary conditions with non-vanishing resultants along the edges.

† The consequence is that a matrix equivalent to the typical stiffness matrix, which will be constructed later, becomes symmetric.

To overcome this mathematical problem, many various forms of base functions have been examined. The final form, we have selected, is quite simple:

$$\phi(x,y) = \sum_{i=1}^{N_s} \phi^{(i)}(x_i, y_i) \tag{13a}$$

$$\phi^{(i)}(x_i, y_i) = A_0^{(i)}\left[\left(\frac{x_i}{L_i} - \frac{1}{2}\right)^2 - \left(\frac{y_i}{L_i}\right)^2\right] + \sum_{n=1}^{N_h} A_n^{(i)} \cos\frac{n\pi}{L_i} x_i \exp\left(-\frac{n\pi}{L_i} y_i\right). \tag{13b}$$

Some remarks are to be made regarding the present choice. The base functions satisfy the governing equation exactly and the terms associated with $A_0^{(i)}$ are non-decaying functions. Perhaps, the novel features of the present technique are the *combined use of polynomials and Fourier series type solutions*, and the *form of the selected polynomials*. Although the form (13b) looks quite simple, most time in this work has been spent on finding the correct form of the base functions given here.

It is worthwhile to state the criteria used to choose appropriate base functions.

(1) The base functions must satisfy the governing equation for computational effectiveness.
(2) When ϕ is prescribed on all edges, the solution must be unique.
(3) When $\partial\phi/\partial v$ is prescribed on all edges, the solution must be unique up to a constant and the trial functions must satisfy eqn (5).
(4) The same form should be able to be used for all edges.
(5) Low-order polynomials are preferred for numerical efficiency.

Besides the polynomials $(x_i/L_i - 1/2)^2 - (y_i/L_i)^2$ given in eqn (13b), some other simple polynomials which satisfy the governing equation exactly have also been examined:

$$1, \quad x_i, \quad y_i, \quad x_i^2 - y_i^2, \quad x_i y_i. \tag{14}$$

Interestingly enough, none of the polynomials in eqn (14) satisfies the criteria (2) and/or (3). The proof has been done analytically for equilateral triangular, and rectangular domains. However, for general geometries, the satisfaction of the criteria (2) and (3) is checked numerically, which will be discussed later. Condition (4) is not a mathematical requirement, but it is imposed for simpler and more efficient formulation. It is interesting that the polynomials $(x_i/L_i)^2 - (y_i/L_i)^2$ do not satisfy condition (2). With the addition of a constant to $(x_i/L_i)^2 - (y_i/L_i)^2$, $(x_i/L_i)^2 - (y_i/L_i)^2 + 1$ can also satisfy condition (2). But a further modification to $(x_i/L_i - 1/2)^2 - (y_i/L_i)^2$ is shown to be converging faster in numerical computation due to the symmetry nature about x_i.

The restriction in the present approach is that the base functions in eqn (13) work for up to pentagonal domains. This is because only the functions, $\{1, X, Y, X^2 - Y^2$ and $XY\}$ (where (X, Y) denotes the global coordinates) can be generated by the present base functions associated with $A_0^{(i)}$ $(i = 1, \ldots, N_s)$, and the present polynomials loose functional independence for polygonal domains with more than 5 edges. Although the correct form of higher order polynomials may be found to handle the domain with more than 5 edges, the method would not be simple or efficient. Thus, general domains are divided into super elements, such as triangular, quadrilateral or pentagonal, and the extension to more general cases will be given in the next section.

When either ϕ or $\partial\phi/\partial v$ is prescribed along the edges of the boundary, the unknown coefficients $A_n^{(i)}$ $(n = 0, \ldots, N_h, i = 1, \ldots, N_s)$ in eqn (13b) must be determined. Since the boundary conditions are to be expressed in the form of the Fourier cosine series given in eqns (8) and (9), the coefficient relation between $(W_n^{(i)}, F_n^{(i)})$ and $A_n^{(i)}$ will be needed.

The results can be written in compact form as:

$$\tilde{\mathbf{W}} = \mathbf{WM} \cdot \mathbf{A} \tag{15a}$$

$$\tilde{\mathbf{F}} = \mathbf{FM} \cdot \mathbf{A} \tag{15b}$$

where

$$\tilde{\mathbf{W}} = \begin{Bmatrix} \tilde{\mathbf{W}}^{(1)} \\ \tilde{\mathbf{W}}^{(2)} \\ \vdots \\ \tilde{\mathbf{W}}^{(N_s)} \end{Bmatrix}; \quad \tilde{\mathbf{F}} = \begin{Bmatrix} \tilde{\mathbf{F}}^{(1)} \\ \tilde{\mathbf{F}}^{(2)} \\ \vdots \\ \tilde{\mathbf{F}}^{(N_s)} \end{Bmatrix}; \quad \mathbf{A} = \begin{Bmatrix} \mathbf{A}^{(1)} \\ \mathbf{A}^{(2)} \\ \vdots \\ \mathbf{A}^{(N_s)} \end{Bmatrix} \tag{16a}$$

and

$$\tilde{\mathbf{W}}^{(i)} = \begin{Bmatrix} \tilde{W}_0^{(i)} \\ \tilde{W}_1^{(i)} \\ \vdots \\ \tilde{W}_{N_h}^{(i)} \end{Bmatrix}; \quad \tilde{\mathbf{F}}^{(i)} = \begin{Bmatrix} \tilde{F}_0^{(i)} \\ \tilde{F}_1^{(i)} \\ \vdots \\ \tilde{F}_{N_h}^{(i)} \end{Bmatrix}; \quad \mathbf{A}^{(i)} = \begin{Bmatrix} A_0^{(i)} \\ A_1^{(i)} \\ \vdots \\ A_{N_h}^{(i)} \end{Bmatrix} \tag{16b}$$

and the matrices **WM** and **FM** are simpler to construct from their submatrices $\mathbf{WM}^{(i,j)}$ and $\mathbf{FM}^{(i,j)}$:

$$\mathbf{WM} = \begin{bmatrix} \mathbf{WM}^{(1,1)} & \mathbf{WM}^{(1,2)} & \dots & \mathbf{WM}^{(1,N_s)} \\ \mathbf{WM}^{(2,1)} & \mathbf{WM}^{(2,2)} & \dots & \mathbf{WM}^{(2,N_s)} \\ \dots & & & \\ \mathbf{WM}^{(N_s,1)} & \mathbf{WM}^{(N_2,2)} & \dots & \mathbf{WM}^{(N_s,N_s)} \end{bmatrix} \tag{17a}$$

$$\mathbf{FM} = \begin{bmatrix} \mathbf{FM}^{(1,1)} & \mathbf{FM}^{(1,2)} & \dots & \mathbf{FM}^{(1,N_s)} \\ \mathbf{FM}^{(2,1)} & \mathbf{FM}^{(2,2)} & \dots & \mathbf{FM}^{(2,N_s)} \\ \dots & & & \\ \mathbf{FM}^{(N_s,1)} & \mathbf{FM}^{(N_2,2)} & \dots & \mathbf{FM}^{(N_s,N_s)} \end{bmatrix}. \tag{17b}$$

The matrices $\mathbf{WM}^{(i,j)}$ and $\mathbf{FM}^{(i,j)}$ denote the contributions of the base functions $\phi^{(j)}$ associated with the jth edge on the ith edge. It is important to note that the components of the submatrices $\mathbf{WM}^{(i,j)}$ are found in closed form from the following definition:

$$\left[\left(\frac{x_j}{L_j} - \frac{1}{2}\right)^2 - y_j^2\right]_{y_i=0} = WM_{(0,0)}^{(i,j)} + \sum_{n=1}^{N_h} WM_{(n,0)}^{(i,j)} \cos(\lambda_n^{(i)} x_i) \tag{18a}$$

$$[\cos \lambda_m^{(j)} \exp(-\lambda_m^{(j)} y_j)]_{y_i=0} = WM_{0,m}^{(i,j)} + \sum_{n=1}^{N_h} WM_{(n,m)}^{(i,j)} \cos(\lambda_n^{(i)} x_i) \quad (m \geqslant 1) \tag{18b}$$

where $\lambda_n^{(i)} = n\pi/L_i$ and $\lambda_m^{(j)} = m\pi/L_j$, and L_i stands for the length of the ith edge. Similarly,

$$\left\{\frac{\partial}{\partial y_i}\left[\left(\frac{x_j}{L_j} - \frac{1}{2}\right)^2 - \left(\frac{y_j}{L_j}\right)^2\right]\right\}_{y_i=0} = \frac{FM_{(0,0)}^{(i,j)}}{2} + \sum_{n=1}^{N_h} FM_{(n,0)}^{(i,j)} \cos(\lambda_n^{(i)} x_i) \tag{19a}$$

$$\left[\frac{\partial}{\partial y_i} \cos \lambda_m^{(j)} \exp(-\lambda_m^{(j)} y_j)\right]_{y_i=0} = \frac{FM_{0,m}^{(i,j)}}{2} + \sum_{n=1}^{N_h} FM_{(n,m)}^{(i,j)} \cos(\lambda_n^{(i)} x_i) \quad (m \geqslant 1). \tag{19b}$$

In order to differentiate the function defined in the jth local coordinates with respect to the ith local coordinates, one can simply use the chain rule:

$$\left[\frac{\partial \phi^{(j)}(x_j, y_j)}{\partial y_i}\right]_{y_i=0} = \left[\frac{\partial \phi^{(j)}(x_j, y_j)}{\partial x_j}\frac{\partial x_j}{\partial y_i} + \frac{\partial \phi^{(j)}(x_j, y_j)}{\partial y_j}\frac{\partial y_j}{\partial y_i}\right]_{y_i=0}$$

where $\partial x_j/\partial y_i$ and $\partial y_j/\partial y_i$ denote the coordinate relations. It should be emphasized again here that all the elements $WM^{(i,j)}_{(n,m)}$ and $FM^{(i,j)}_{(n,m)}$ are obtained in closed form without any numerical integration.

The satisfaction of criteria (2) and (3) stated earlier can be checked by examining the rank of **WM** and **FM**. Namely, the rank of **WM** must be equal to the dimension of **WM**, and the rank of **FM** must be equal to 1 less than the dimension of **FM** due to eqn (5).

4. FORMULATION IN MULTIPLY CONNECTED REGIONS

In the previous section, the analysis is limited to general convex polygonal regions, up to pentagonal. For other regions, they are subdivided into convex regions as shown in Fig. 2. Between the divided elements, the continuity relations must be used to form the final sets of equations. To this end, it is convenient to form an element matrix $\mathbf{KM}_e$, which relates the warping displacement and its normal derivative along the boundary:

$$\tilde{\mathbf{F}}_e = \mathbf{KM}_e \cdot \tilde{\mathbf{W}}_e \tag{20a}$$

$$\mathbf{KM}_e = \mathbf{FM}_e \cdot \mathbf{WM}_e^{-1} \tag{20b}$$

where the subscript e is used to designate the quantities defined for each element, and $\tilde{\mathbf{F}}_e$ and $\tilde{\mathbf{W}}_e$ are the quantities defined in eqn (16) along the edges of an element.

For consistent sign convention, the element edges are always numbered counterclockwisely. Considering the symmetry nature of the Fourier cosine series and the orientation of the adjacent local coordinates, one can show that the continuity conditions along the adjacent edges, in terms of the Fourier cosine series coefficients, are expressed as

$$\tilde{W}^{(j)}_k = \begin{cases} \tilde{W}^{(i)}_k & (k = 0, 2, 4, \ldots) \\ -\tilde{W}^{(i)}_k & (k = 1, 3, \ldots) \end{cases} \tag{21a}$$

and

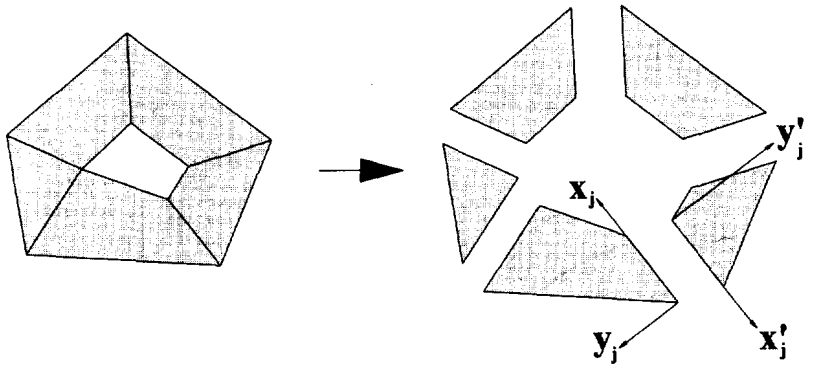

(a) **(b)**

Fig. 2. The multiply connected cross section shown in (a) is subdivided into several convex cross sections as suggested in (b).

$$\tilde{F}_k^{(j)} = \begin{cases} -\tilde{F}_k^{(j')} & (k = 0, 2, 4, \ldots) \\ \tilde{F}_k^{(j')} & (k = 1, 3, \ldots) \end{cases} \tag{21b}$$

where the primed quantities are those associated with the adjacent element. Except that the signs in eqn (21) are carefully selected, the assembling procedure to form the global matrix $\mathbf{KM}_g$ defined below is almost identical to that used in the finite element analysis; there is no need to explain the assembling procedure in detail. The results is

$$\tilde{\mathbf{F}}_g = \mathbf{KM}_g \cdot \tilde{\mathbf{W}}_g \tag{22}$$

$$\mathbf{KM}_g = \sum_{e=1}^{N_e} \mathbf{KM}_e; \quad \tilde{\mathbf{W}}_g = \sum_{e=1}^{N_e} \tilde{\mathbf{W}}_e; \quad \tilde{\mathbf{F}}_g = \sum_{e=1}^{N_e} \tilde{\mathbf{F}}_e. \tag{23}$$

In eqns (22, 23), the subscript g stands for the globally assembled quantities and N_e denotes the total number of subdivided elements.

To summarize the critical features of the present method, (1) the domain size of each element can be arbitrarily large and (2) the base functions satisfy the governing differential equation exactly. Therefore the present method is very effective in terms of modeling efforts and the amount of numerical calculation.

5. NUMERICAL EXAMPLES

The first example considered is a bar with the equilateral cross section of altitude $3a$ shown in Fig. 3, for which the exact solution is known (Sokolnikoff, 1956). The exact value of the torsional rigidity D is given by $D/G = 9\sqrt{3}a^4/5$. The present results are compared with the exact solution and the ANSYS results, for the case of $a = 1$.

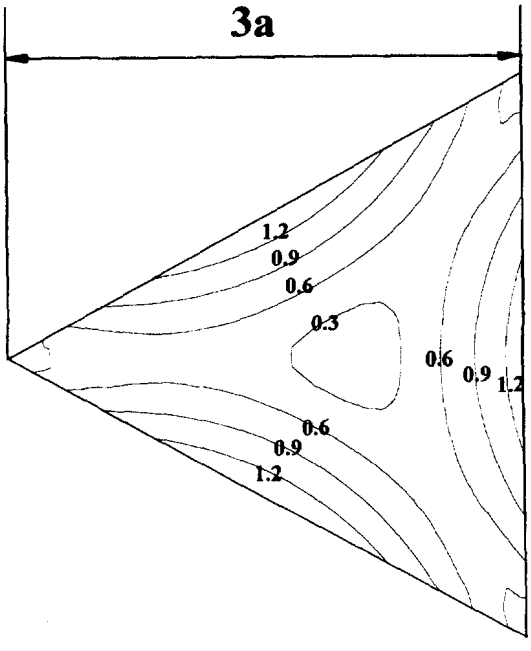

Fig. 3. The equilateral triangular cross section of altitude $3a$. The contour of equivalent stress (σ_{eq}) obtained for the present method is shown.

Table 1. The values of D/G for the bar($a = 1$) shown in Fig. 3. (N_h = the highest harmonic number, N_{el} = the number of finite elements used for ANSYS)

Present with $N_e = 1$	ANSYS	Exact
3.115 ($N_h = 4$)	3.087 ($N_{el} = 175$)	3.117
3.116 ($N_h = 8$)	3.110 ($N_{el} = 300$)	3.117
3.117 ($N_h = 16$)	3.114 ($N_{el} = 675$)	3.117

Table 2. The maximum equivalent stress $\sigma_{eq}|_{max}$ ($\sigma_{eq} = \sqrt{\sigma_{zx}^2 + \sigma_{zy}^2}/G$) for the bar shown in Fig. 3

Present with $N_e = 1$	ANSYS	Exact
1.493 ($N_h = 4$)	1.300 ($N_{el} = 175$)	1.500
1.499 ($N_h = 8$)	1.399 ($N_{el} = 300$)	1.500
1.500 ($N_h = 16$)	1.433 ($N_{el} = 675$)	1.500

It is apparent from Table 1 that the present results converge very rapidly to the exact value only with a small number of terms, and the ANSYS finite element results converge favorably. Table 2 lists the numerical results for the maximum value of the equivalent stress $\sigma_{eq} = \sqrt{\sigma_{zx}^2 + \sigma_{zy}^2}/G$, and one can see that the present results converge extremely fast in comparison with ANSYS results. The equivalent stress contours obtained from the present analysis and the exact solutions are compared, and the two results are found to be virtually undistinguishable. Therefore, only the present results are shown in Fig. 3.

As the second example, a bar with a pentagonal cross section is considered. Since no exact solution is known, the present results for the torsional rigidity and stress are compared in Tables 3 and 4 with finite element results. For the torsional rigidity, the finite element result converges as fast as the present result but it is apparent that slower and less accurate results are obtained from the finite element analysis for the stress. Figure 4 shows the stress distribution obtained from the present method, which is confirmed to be almost identical to the ANSYS result although the ANSYS results is not plotted here.

Next, a rectangular bar with a rectangular hole under torsion is analysed. As shown in Fig. 5, the region is subdivided into only 8 large elements ($N_e = 8$). The present converging results for the torsional rigidity with $N_h = 17$ are compared with the ANSYS results as the function of eccentricity, ε, which is defined as $\varepsilon = (d-c)/c$, in Fig. 6. As many as 3600 elements are needed in the ANSYS calculation to obtain results comparable to the present results.

Table 3. The values of D/G for the bar shown in Fig. 4

Present with $N_e = 1$	ANSYS
0.441 ($N_h = 4$)	0.440 ($N_{el} = 225$)
0.442 ($N_h = 8$)	0.441 ($N_{el} = 900$)
0.442 ($N_h = 16$)	0.442 ($N_{el} = 3600$)

Table 4. The maximum stress $\sigma_{eq}|_{max}$ for the bar shown in Fig. 4

Present with $N_e = 1$	ANSYS
0.856 ($N_h = 4$)	0.816 ($N_{el} = 225$)
0.871 ($N_h = 8$)	0.834 ($N_{el} = 900$)
0.875 ($N_h = 16$)	0.847 ($N_{el} = 3600$)

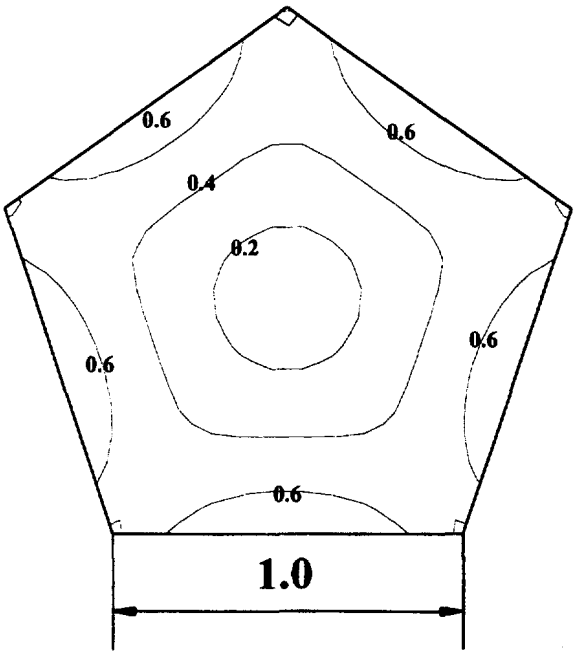

Fig. 4. The equilateral pentagonal cross section with edge length of '1'. The contour of equivalent stress (σ_{eq}) obtained for the present method is shown.

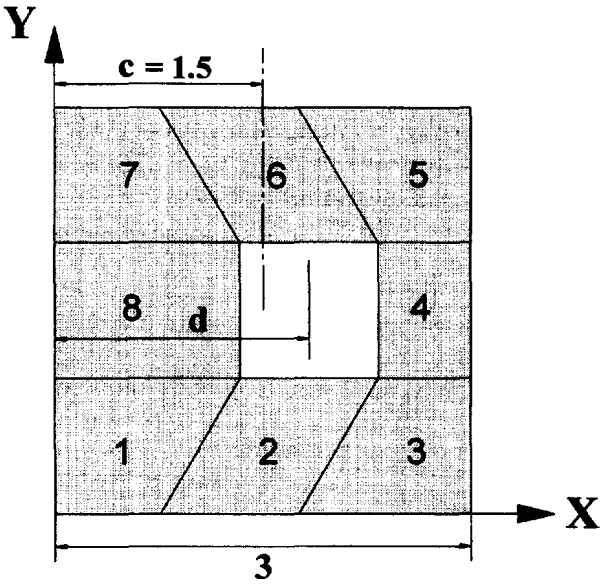

Fig. 5. A rectangular bar with an inner rectangular hole.

6. CONCLUSIONS

In this paper, the torsion problem in bars with multiply connected cross sections is solved by a modified Fourier series method utilizing polynomials as well as the Fourier cosine series both of which satisfy the governing equation exactly. The present combination of polynomials and series solutions and the proposed form of the polynomials are shown to be very useful. The technique subdividing general cross sections into a few large convex regions is also confirmed to be effective. The number of elements needed in the present technique and the amount of numerical calculations are order of magnitude smaller than those needed in typical finite element methods.

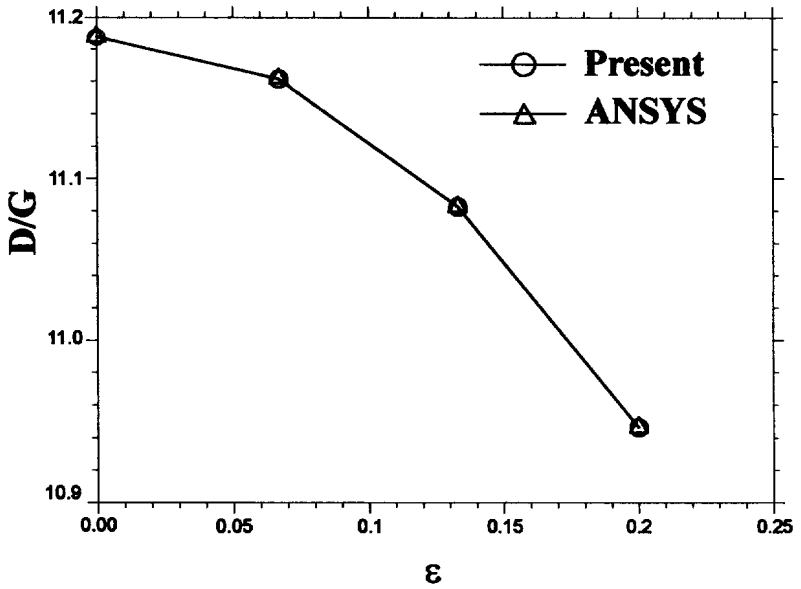

Fig. 6. The variation of D/G for the bar shown in Fig. 5 is shown as the function of the eccentricity $\varepsilon = (d-c)/c$.

Acknowledgement—This work was supported by the Turbo and Power Machinery Research Center.

REFERENCES

Bird, M. and Steele, C. R. (1992) A solution procedure for Laplace's equation on multiply connected circular domains. *Journal of Applied Mechanics* **59,** 398–404.

Ie, C. A. and Kosmatka, J. B. (1992) On the analysis of prismatic beams using first-order warping functions. *International Journal of Solids and Structures* **29,** 879–891.

Irschik, H. (1991) Analogies between bending of plates and torsion problem. *Journal of Engineering Mechanics* **117,** 2503–2508.

Kang, L. C. (1992) A Fourier series method for polygonal domains; large element computation for plates. PhD thesis, Stanford University, Stanford, California.

Kang, L. C., Wu, C. H. and Steele, C. R. (1995) Fourier series for polygonal plate bending; a very large plate element. *Applied Mathematics and Computation* **67,** 197–225.

Mason, W. E., Jr. and Herrmann, L. R. (1968) Elastic shear analysis of general prismatic beams. *ASCE Journal of Engineering Mechanics Division* **94,** 965–983.

Rand, O. (1992) Exact solution for general torsion problems using boundary singularities. *Journal of Engineering Mechanics* **118,** 2141–2147.

Sokolnikoff, I. S. (1956) *Mathematical Theory of Elasticity*. McGraw Hill Book Co., New York.

Timoshenko, S. P. (1982) *Theory of Elasticity*. McGraw Hill Book Co., New York.